

Supplementary Information for

Metabolism modulates network synchrony in the aging brain

Corey Weistuch, Lilianne R Mujica-Parodi, Rostam M Razban, Botond Antal, Helena van Nieuwenhuizen, Anar Amgalan and Ken A Dill

Ken A Dill.
E-mail: dill@laufercenter.org

This PDF file includes:

Supplementary text
Figs. S1 to S6 (not allowed for Brief Reports)
SI References

Supporting Information Text

Derivation of the Ising model of fMRI network synchrony

Here we apply the *Principle of Maximum Entropy* to derive the Ising model of the fMRI network synchrony s , a measure of brain-wide coordination. Maximum entropy provides a rigorous machinery for inferring minimally-biased probability distributions from limited information (1). Here, this distribution is over network configurations c , consisting of the binary (-1 or $+1$) states of each brain region. As is typical practice, our information consists of the mean (0) and variance of synchrony $Var(s)$ and thus considers up to pairwise interactions between brain regions (2). The entropy of a given distribution of configurations $P(c)$ is then given as:

$$S\{P\} = - \sum_c P(c) \ln P(c) + \mu \sum_c P(c) + N^2 \lambda \sum_c s(c)^2 P(c) \quad [1]$$

Here, λ reflects the average interaction across all (N^2) pairs of brain regions and is used to enforce the total variability in synchrony observed in the data. Similarly, μ enforces the normalization of $P(c)$. Maximizing this entropy, we find that the optimal model is given by:

$$P(c) = e^{-1+\mu+N^2\lambda s(c)^2} \quad [2]$$

To satisfy the normalization constraint, we additionally require:

$$e^{-1+\mu} \sum_c e^{N^2\lambda s(c)^2} = 1 \implies e^{1-\mu} = \sum_c e^{N^2\lambda s(c)^2} = Z \quad [3]$$

where the last equality is the definition of the partition function Z of the maximum entropy distribution. Therefore:

$$P(c) = Z^{-1} e^{N^2\lambda s(c)^2} \quad [4]$$

Finally, the probability of each synchrony s is given by:

$$P(s) = \sum_{c:s(c)=s} P(c) = Z^{-1} \binom{N}{N(1+s)/2} e^{N^2\lambda s^2} \quad [5]$$

Validation of the Ising model

Testing the Model Assumptions. Our use of the Ising model requires two assumptions about the data. First, it assumes that fMRI signals (in particular their correlations) are preserved after binarization (through BDM). Second, our use of a global coupling parameter Λ assumes that brain regions are fully-connected and positively correlated. To test the first assumption, we utilized the lifespan Cam-CAN fMRI dataset ($N = 642$, see Methods) to compare the functional connectivities (FC) computed from both the raw and binarized signals. To test the strength of the association between these two FC estimates, we randomly selected intervals of a fixed length (*Window Size*) and computed the correlation between the FC estimates (averaged across regions) from each subject. We consistently found a strong correlation (Pearson $r > 0.75$) between these estimates across all subjects, suggesting that binarization does indeed preserve FC (**Fig. S1A**). In addition, we found that the strength of this association (using a window size of 260 TR) did not depend on age (**Fig. S1B**), ensuring that BDM binarization is valid across our population of interest.

To verify that FC is typically positive between pairs of brain regions, we next computed the average FC (over pairs of regions and over Cam-CAN subjects) across our original 498 regions. **Fig. S2** shows the histogram (over regions) of these average FC values and illustrates that (other than a few outlier regions with negative average FC values) most regions are positively correlated (with average FC ≈ 0.2). To satisfy the assumptions of our model, we thus restricted analysis to the top 100 regions whose average correlations were both positive and dependent on age (see Methods: Model Fitting). However, **Fig. S3**, which replicates our analysis (**Fig. 5A**) for $N = 10$ and $N = 50$ regions, illustrates that our results are robust to this choice.

Verifying the Model Predictions. The Ising model predicts that the distribution of synchrony $P(s)$ abruptly switches from a unimodal to a bimodal shape at the critical point $\Lambda = 0$. **Fig. S4** shows the distributions of synchrony (Orange) observed in a representative set of subjects (from Cam-CAN and the *PAGB* Bolus study) compared to the Ising model (Blue). Likely due to residual noise in the raw fMRI signals, the Ising model consistently underestimates the observed frequencies of zero synchrony. Nevertheless, the Ising model broadly agrees with the data. Most importantly, the Ising model correctly predicts the emergence of a bimodal (or broad, due to the aforementioned deviation) distribution of synchrony

Establishing Biological Significance. In contrast to other imaging modalities, such as magnetoencephalography (MEG), fMRI provides only indirect evidence of neural activity. Using the matched fMRI-MEG provided by Cam-CAN, we next sought to identify direct neural correlates with the Ising coupling, Λ . **Fig. S5** illustrates the significant correlation ($p = 2.2 \times 10^{-4}$, $N = 589$) between Λ (as derived from fMRI) and Global Coherence (a metric of functional connectivity as derived from MEG (3)) and thus provides preliminary evidence of a neural mechanism underlying our results. However, both fMRI and MEG are susceptible to artifacts induced by subject head motion, which, in turn, are often more prominent in older subjects. As further validation for the biological significance of our findings, however, **Fig. S6** shows that subject head motion does not correlate with Λ in both the Cam-CAN and HCP-A datasets.

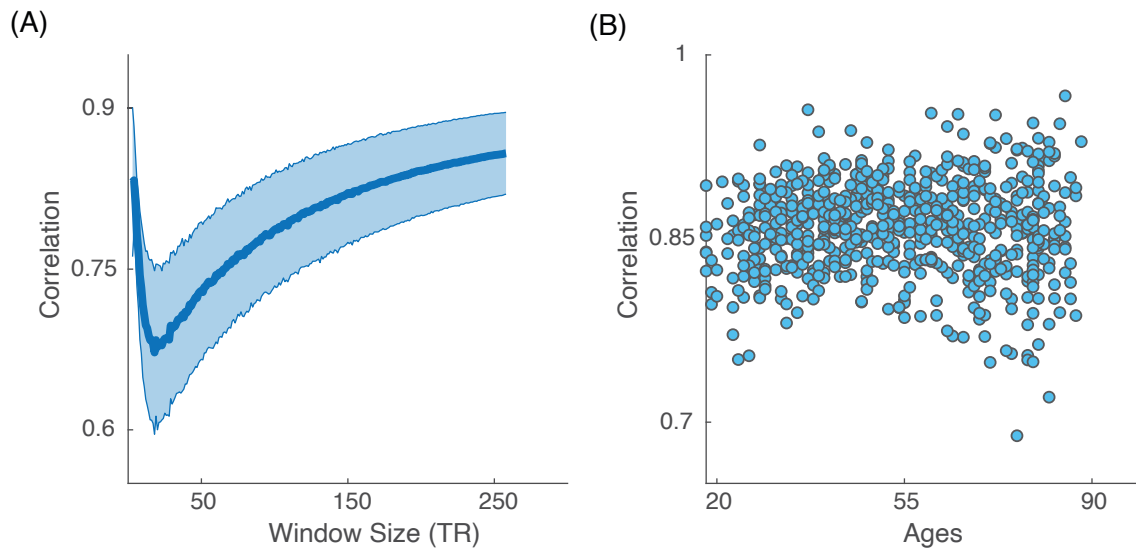


Fig. S1. Functional connectivity (FC) can be recovered from simple, binarized signals (BDM). (A) The correlation between FC calculated using raw and binarized data averaged across different windows of time. Error bars represent the population standard deviation ($N = 642$). (B) The same correlations (using the maximum window size) plotted against age.

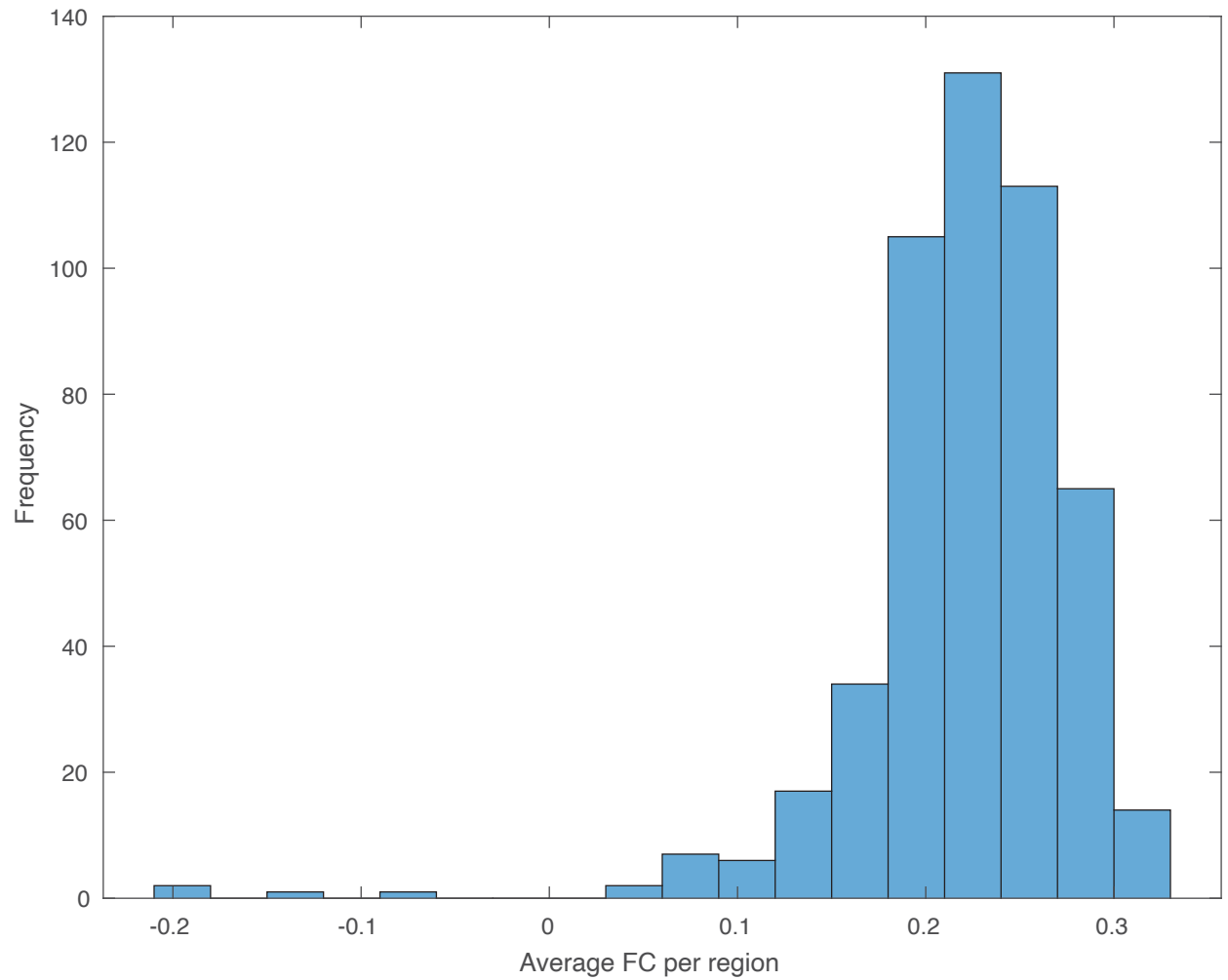


Fig. S2. Resting-state functional regions are globally correlated. Shown is the population-averaged ($N = 642$ subjects) functional connectivity of each region (498 in total, averaged over the remaining 497 pairs). This justifies our use of a globally-connected network model.

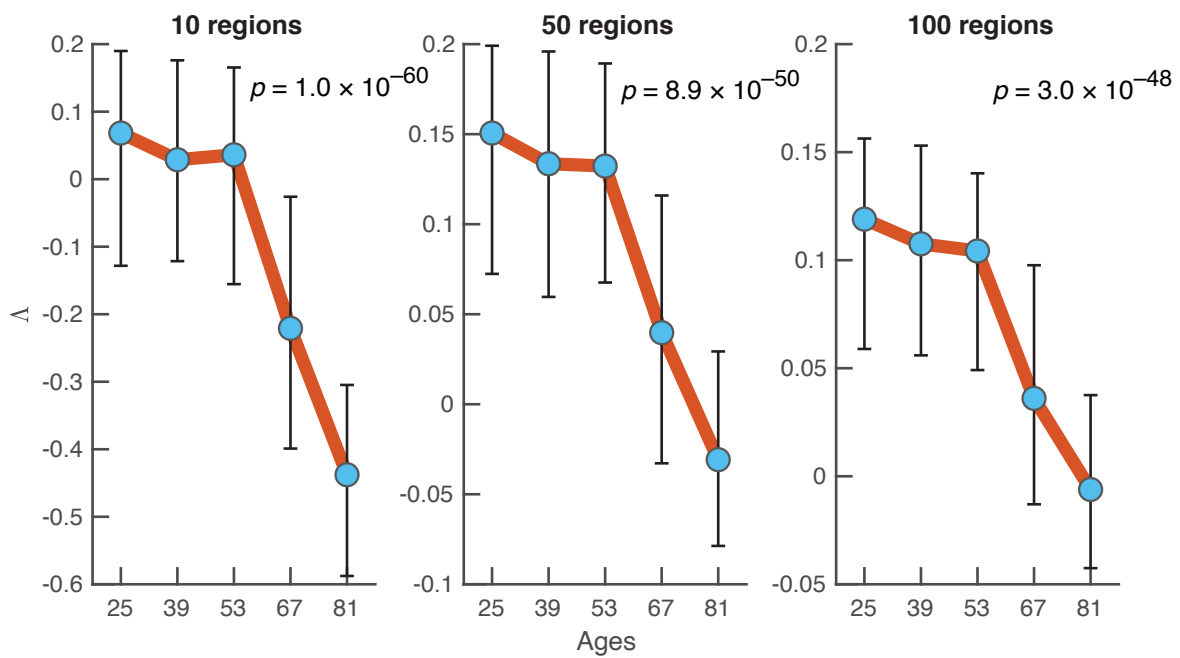


Fig. S3. Δ decreases with age and traverses the critical point, regardless of the number of regions selected (N). Functional regions were selected, as in Methods: Model fitting, by identifying the $N = 10, 50,$ and 100 regions with the largest decreases in average FC with age.

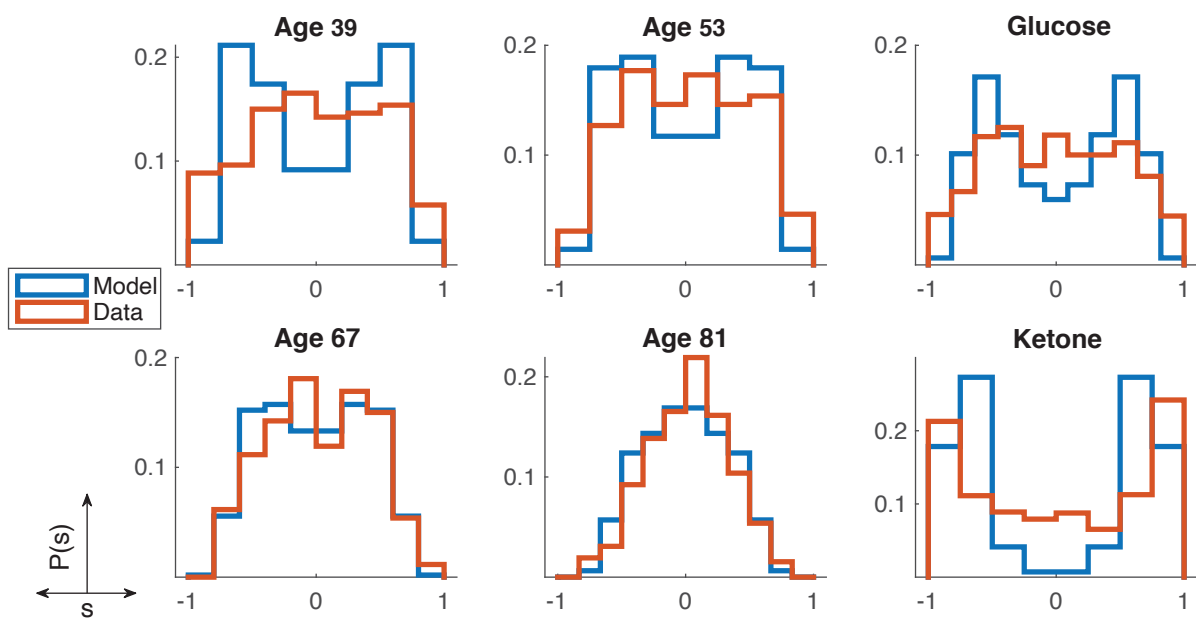


Fig. S4. The Ising model (blue) accurately describes the distribution of synchronies extracted from functional data (orange). Shown are sample fits of the distribution of synchronies $P(s)$ from randomly chosen subjects in each age group (Cam-CAN) and metabolic condition (PAGB Bolus).

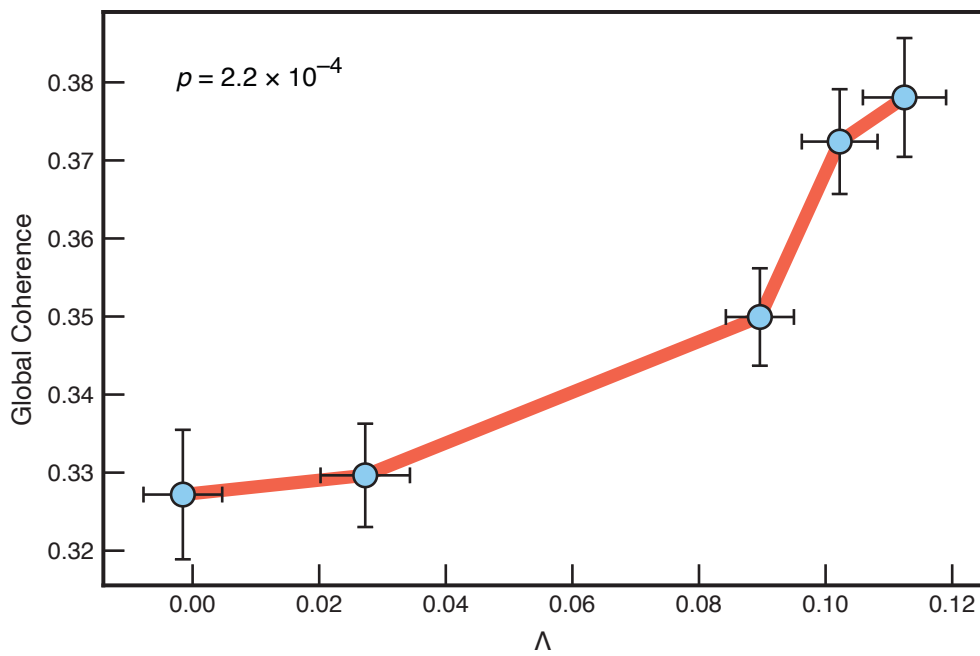


Fig. S5. Global coherence (a metric of functional connectivity as computed in (3)) in the alpha (8 - 12 Hz) band of resting state MEG increases as a function of Λ ($p = 2.2 \times 10^{-4}$, Spearman-rank permutation test). Global coherences were calculated using lifespan resting state MEG data available via the Cam-CAN data repository (4, 5), using the same subjects used in the calculations of Λ . Comparison between Λ and coherence was then performed on subjects having both modalities available ($N = 589$). The data were binned into age brackets of 14 years and averaged for visualization purposes. Error bars are the standard error of the mean.

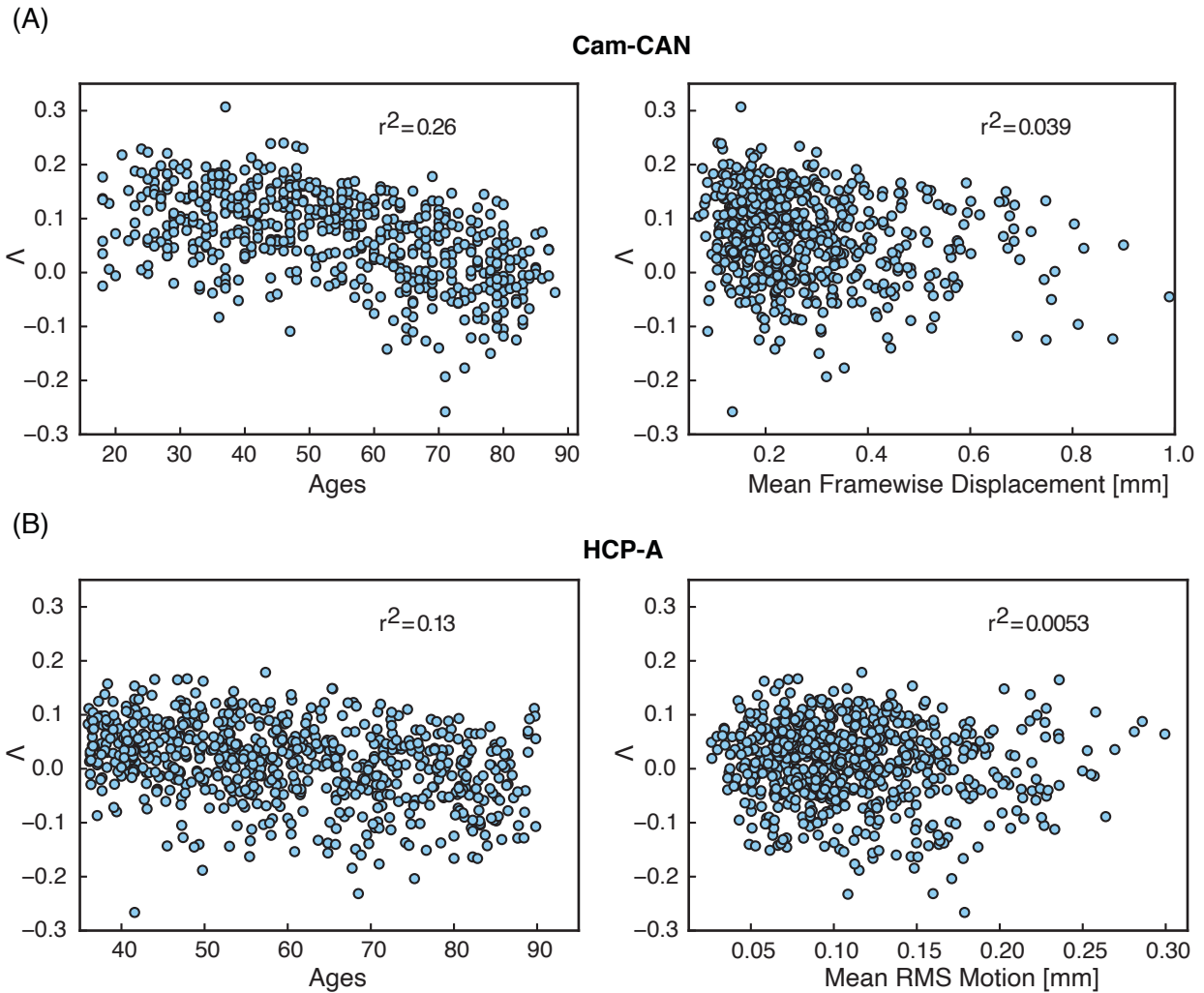


Fig. S6. Variance in head motion did not explain the observed trends in synchrony, as demonstrated across multiple datasets. In order to address the possibility of head motion being the underlying driver mechanism behind changes in network synchrony, we quantified linear correlations between Head Motion and synchrony for both Cam-CAN (A) and HCP-A (B) datasets. To compare the motion related association with that of age, we also displayed the relationship between age and synchrony. As shown, motion related effects seemed to be non-existent, as opposed to the age-synchrony relationship, where the association was robust. These results demonstrate that in the case of synchrony, head motion would not correlate with effects observed across age, even despite the fact that head motion is generally correlated with age.

References

1. ET Jaynes, Information theory and statistical mechanics. *Phys. review* **106**, 620 (1957).
2. E Schneidman, MJ Berry, R Segev, W Bialek, Weak pairwise correlations imply strongly correlated network states in a neural population. *Nature* **440**, 1007–1012 (2006).
3. B Sahoo, A Pathak, G Deco, A Banerjee, D Roy, Lifespan associated global patterns of coherent neural communication. *Neuroimage* **216**, 116824 (2020).
4. MA Shafto, et al., The cambridge centre for ageing and neuroscience (cam-can) study protocol: a cross-sectional, lifespan, multidisciplinary examination of healthy cognitive ageing. *BMC neurology* **14**, 25 (2014).
5. JR Taylor, et al., The cambridge centre for ageing and neuroscience (cam-can) data repository: structural and functional mri, meg, and cognitive data from a cross-sectional adult lifespan sample. *Neuroimage* **144**, 262–269 (2017).